Journal of Chromatography A, 1490 (2017) 47–53

Contents lists available at ScienceDirect

Journal of Chromatography A

journal homepage: www.elsevier.com/locate/chroma

Nickel-Salen supported paramagnetic nanoparticles for 6-His-target recombinant protein affinity purification

Zahra Rashid[a], Ramin Ghahremanzadeh[b], Mohammad-Reza Nejadmoghaddam[b,c], Mahboobeh Nazari[b], Mohammad-Reza Shokri[d], Hossein Naeimi[a,*], Amir-Hassan Zarnani[e,f,*]

[a] Department of Organic Chemistry, Faculty of Chemistry, University of Kashan, Kashan, Iran
[b] Nanobiotechnology Research Center, Avicenna Research Institute, ACECR, Tehran, Iran
[c] Nanotechnology Research Center, Faculty of Pharamcy, Tehran University of Medical Sciences (TUMS), Tehran, Iran
[d] Department of Immunology, Faculty of Medicine, Iran University of Medical Sciences, Tehran, Iran
[e] Department of Immunology, School of Public Health, Tehran University of Medical Science, Tehran, Iran
[f] Immunology Research Center, Iran University of Medical Sciences, Tehran, Iran

ARTICLE INFO

Article history:
Received 13 December 2016
Received in revised form 8 February 2017
Accepted 9 February 2017
Available online 13 February 2017

Keywords:
Magnetic nanoparticles
Protein purification
Immobilized metal affinity chromatography (IMAC)
Histidine-tagged protein
Salen-type ligands

ABSTRACT

In this research, a simple, efficient, inexpensive, rapid and high yield method for the purification of 6 × histidine-tagged recombinant protein was developed. For this purpose, manganese ferrite magnetic nanoparticles (MNPs) were synthesized through a co-precipitation method and then they were conveniently surface-modified with tetraethyl orthosilicate (TEOS) in order to prevent oxidation and form high density of hydroxyl groups. Next, the salen ligand was prepared from condensation reaction of salicylaldehyde and 3-aminopropyl (trimethoxy) silane (APTMS) in 1:1 molar ratio; followed by complexation with $Ni(OAc)_2.4H_2O$. Finally, the prepared Ni(II)-salen complex conjugated to silica coated MNPs and $MnFe_2O_4$@SiO_2@Ni-Salen complex nanoparticles were obtained. The functionalized nanoparticles were spherical with an average diameter around 70 nm. The obtained MNPs had a saturation magnetization about 54 emu/g and had super paramagnetic character. These MNPs were used efficiently to enrich recombinant histidine-tagged (His-tagged) protein-A from bacterial cell lysate. In about 45 min, highly pure His-tagged recombinant protein was obtained, as judged by SDS-PAGE analysis and silver staining. The amount of target protein in flow through and washing fractions was minimal denoting the high efficiency of purification process. The average capacity of the matrix was found to be high and about 180 ± 15 mg g^{-1} (protein/$MnFe_2O_4$@SiO_2@Ni-Salen complex). Collectively, purification process with $MnFe_2O_4$@SiO_2@Ni-Salen complex nanoparticles is rapid, efficient, selective and whole purification can be carried out in only a single tube without the need for expensive systems.

1. Introduction

In parallel with the revolutionary improvement of techniques for efficient expression of recombinant proteins, there is an ever-increasing need for simple, fast and convenient protein purification methods which allow for direct isolation of proteins from cell lysates. Purification of recombinant proteins is an essential step for studying the structure and function of proteins, and for therapeutic and diagnostic applications. Affinity separations based on affinity tags that exploit the unique property of extremely specific biological interactions to achieve separation and purification is theoretically capable of giving robust purification, even from complex mixtures in a single process. It allows the purification of nearly any protein without prior knowledge of its biochemical properties. A variety of proteins, domains, or peptides have been used as affinity tags to facilitate the purification of interest proteins from crude extracts.

Among the existing protocols, immobilized metal affinity chromatography (IMAC) has been considered as one of the most effective approaches for the separation and purification of recombinant proteins [1]. This procedure is based on the interaction between a transition metal ion (Co^{2+}, Ni^{2+}, Cu^{2+}, and Zn^{2+}) immobilized on a matrix and specific amino acid side chains as electron donor groups located on the surface of proteins [2–4]. Everson and

* Correspondings author.
E-mail address: naeimi@kashanu.ac.ir (H. Naeimi).

http://dx.doi.org/10.1016/j.chroma.2017.02.014
0021-9673/

Parker firstly used immobilization of chelating compounds for the separation of metalloproteinase [5]. IMAC technique became popular through the research work of Porath [6,7] and Sulkowski [8,9] who laid the foundations of the technique that is widely used today and applicable for a variety of purposes, including analytical and preparative purification of proteins, as well as being a valuable tool for studying surface accessibility of certain amino acid residues. IMAC techniques were initially used for separating proteins and peptides with natural histidine residues. The work of Hochuli et al. [10] pioneered the efficient purification of recombinant proteins with engineered histidine affinity handles attached to the N- or C-terminus, especially in combination with the Ni (II)–nitrilotriacetic acid (Ni–NTA) matrix.

The poly-histidine tag (usually 6 × histidine-tagged) is one of the most often used affinity tags [11,12]. The 6 × histidine-tagged comprises six consecutively placed histidine residues incorporated into the C-terminus, N-terminus or both ends of a recombinant protein of interest without impairing their function due to its small size, and the tagged proteins can be purified with no extra expensive reagents or complicated treatments. The whole purification can be finished in a single capture step using (IMAC) [13–15]. Separation of histidine-tagged proteins typically occurs in columns containing resins modified with Ni^{2+} complexes, often Ni^{2+} nitrilotriacetate (Ni^{2+}-NTA), and these methods are attractive for their high protein loading, mild elution conditions, and easy regeneration of the metal complexes on the resin [16,17]. However, slow intraparticle biomolecule diffusion to binding sites in porous micrometer-sized beads can lead to relatively long processing time that can be problematic when purifying unstable proteins [18].

To address these issues, new purification systems based on magnetic nano-materials have been recently reported [19–21]. MNPs have been extensively used in various fields of biotechnology and biomedicine such as cell and stem cell separation, enzyme immobilization, protein separation and immunoassays [22–27], thanks to combining the structural and functional advantages [28]. MNPs with high surface to volume ratio show enhanced physical and chemical properties and their special magnetic properties allow quick separation from aqueous systems in the presence of an external magnetic field [29]. Their physical and chemical properties can be tuned by controlling chemical compositions and relative size of cores and shells. The specific modification of the particles allows isolation of protein or DNA, as well as magnetic cell separation. However, most commercial magnetic beads are micrometer sized and thus have a limited surface area and binding capacity (typically < 25 mg protein/g of beads) [30].

Recently, several groups have successfully reported synthesis of functionalized MNPs for separation of polyhistidine-tagged proteins [31–33]. For example; Wang et al. synthesized nanostructured Fe_3O_4@$NiSiO_3$ by a facile sol–gel and hydrothermal method for a selective adsorption of a histidine-tagged protein from the mixed-protein solutions [34]. Xu et al. reported growth of poly(2-hydroxyethyl methacrylate) brushes on MNPs and subsequent brush functionalization with nitrilotriacetate-Ni^{+2} yielding magnetic beads selectively able to capture polyhistidine-tagged protein directly from cell extracts [35]. Xie et al. reported the synthesis of Fe_3O_4/Au core/shell nanoparticles modified with Ni^{+2}-NTA to separate histidine-tagged proteins from the mixed-protein solution [36].

The salen-type ligands are Schiff bases, usually prepared by the condensation of a salicylaldehyde with an amine that are used in coordination chemistry and homogeneous catalysis. Salen complex contains salen core and transition metal precursors [37]. In this work, we reported design and preparation of novel MNPs of $MnFe_2O_4$@SiO_2@Ni-Salen complex. Application of these nanoparticles in purification of 6 × histidine-tagged recombinant protein-A, as a model for proteins containing histidine tag, has also been investigated. This protein is a cell wall component of the bacterium *Staphylococcus aureus* that binds specifically to many mammalian immunoglobulins, most markedly IgG and is utilized for oriented immobilization of antibodies from different sources [40].

2. Experimental

2.1. Chemicals

The used chemicals in this study including $MnCl_2{\cdot}4H_2O$, $FeCl_3{\cdot}6H_2O$, NaOH, ammonia aqueous solution, tetraethyl orthosilicate (TEOS), 3-aminopropyl (trimethoxy) silane (APTMS), $Ni(OAc)_2{\cdot}4H_2O$, salicylaldehyde, tryptone, yeast extract, NaCl, kanamycin, isopropyl-β-thiogalactopyranoside (IPTG), Na_2HPO_4, Imidazole, Tris-HCl, glycerol, bromophenol blue, sodium dodecyl sulfate, polyacrylamide, Dithiothreitol, all had purity of ≥99% and were obtained from Fluka, Sigma-Aldrich and Merck.

2.2. Instrumentals

IR spectra were recorded as KBr pellets on a Perkin-Elmer 781 spectrophotometer and an Impact 400 Nicolet FT-IR spectrophotometer (Ohio, USA), (http://www.perkinelmer.com/category/infrared-spectroscopy-FT-IR). X-ray diffraction (XRD) pattern of the as-synthesized material was obtained using a Holland Philips Xpert X-ray powder diffraction (XRD) diffractometer (CuK, radiation, λ = 0.154056 nm), at a scanning speed of 2°/min from 10° to 100° (2θ) (Holland, Company: Panalytical), (http://www.panalytical.com/Xray-diffractometers.htm). Scanning electron microscope (SEM) was performed on a FEI Quanta 200 SEM operated at a 20 kV accelerating voltage (China, Phenom-World)(http://www.phenom-world.com/microscopes/phenom-prox). Thermogravimetric/differential thermal analyses (TG/DTA) were performed on a thermal analyzer with a heating rate of 20 °C min^{-1} over a temperature range of 25–800 °C under flowing compressed N_2 (Perkin Elmer, PYRIS Diamond, Japan)(http://www.perkinelmer.com/category/thermogravimetry-analysis-tga). The magnetic measurement of samples was carried out in a vibrating sample magnetometer (VSM) (4 in., Daghigh Meghnatis Kashan Co., Kashan, Iran), (http://nano.kashanu.ac.ir/fa/gallery/45/PhotoList) at room temperature.

2.3. Synthesis of $MnFe_2O_4$@SiO_2@Ni-Salen complex

2.3.1. Synthesis of $MnFe_2O_4$ nanoparticles

$MnFe_2O_4$ nanoparticles were prepared following the reported standard protocol by co-precipitation of $MnCl_2$ and $FeCl_3$ in water in the presence of sodium hydroxide [38]. Briefly, $MnCl_2{\cdot}4H_2O$ and $FeCl_3{\cdot}6H_2O$ were taken in molar ratio of Mn^{2+}: Fe^{3+} = 1:2 to prepare 0.3 mol L^{-1} metal ion solution of 100 ml containing 0.1 mol L^{-1} Mn^{2+} and 0.2 mol L^{-1} Fe^{3+}, and then was slowly dropped into 100 ml NaOH solution of 3 mol L^{-1} at the preheated temperature of 95 °C. After aging for 2 h with continuous stirring, the mixture was filtered, washed with deionized water and dried at 60 °C for 12 h.

2.3.2. Preparation of silica-supported $MnFe_2O_4$ nanoparticles

For silica coating on the surface of $MnFe_2O_4$ nanoparticles, 0.5 g of $MnFe_2O_4$ nanoparticles were first ultrasonically treated with 50 ml of 0.1 M HCl aqueous solution for 10 min. Thereafter, the MNPs were separated by an external magnet (Madison, WI USA, Promega) and washed with deionized water. Then, the particles were homogeneously dispersed in a mixture of 80 ml ethanol, 20 ml deionized water and 5 ml concentrated ammonia aqueous solution (28%v/v) for 30 min. In the next step, 150 μl TEOS was added drop wise to the above-mentioned mixture. After stirring at room

temperature for 6 h, the product was separated and washed with ethanol and deionized water [39].

2.3.3. General procedure for preparation of the salen ligand

The stoichiometric amount of salicylaldehyde (1 mmol, 0.122 g) in methanol (25 ml) was added drop wise to the solution of APTMS (1 mmol, 0.176 g) in 25 ml methanol to obtain 1:1 molar ratio. The obtained solution is yellow due to the imine formation. Then, the solution was stirred under reflux conditions. The progress of the reaction was followed by thin-layer chromatography (TLC) with ethyl acetate: petroleum ether ratio of 8:2. After completion of the reaction, the resulting salen ligand, as the bright yellow solid, was separated by filtration and washed with ethanol (5 ml) and finally dried in vacuum.

2.3.4. General procedure for the preparation of the salen complex of Ni(II)

$Ni(OAc)_2{\cdot}4H_2O$ (0.248 g, 1 mmol) was added to the solution of the salen ligand (0.651 g, 2 mmol) in methanol (25 ml) and the mixture was refluxed for 24 h. After the completion of complex formation, the solution color was changed to green. The resulting product was filtered and washed with ethanol. Then, the product was purified by recrystallization from ethanol and the pure salen complex was obtained as product.

2.3.5. General procedure for the preparation of $MnFe_2O_4$@SiO_2@Ni-Salen complex

For preparation of the $MnFe_2O_4$@SiO_2@Ni-Salen complex, $MnFe_2O_4$@SiO_2 (1 g) was first ultrasonically dispersed in 25 ml ethanol followed by addition of Salen complex of Ni(II) (1 mmol, in 10 ml ethanol). The mixture was refluxed for 12 h. After stirring, the MNPs were harvested by magnet, washed several times with ethanol to remove unreacted $Ni(OAc)_2$ and dried under vacuum at 50 °C.

2.4. Expression of 6 × histidine-tagged recombinant protein-A in E. coli *and its purification by $MnFe_2O_4$@SiO_2@Ni-Salen complex*

2.4.1. Growth of bacteria and induction of gene expression

Protein-A with 6 × histidine residues in their C-terminus (molecular weight of about 42 kD) was expressed in the bacterial cytosol. The expression plasmid, pET21 was prepared and transformed into E. coli BL21 (DE3) as host strain. A single transformed colony was inoculated into 3 ml of Luria Broth (LB), (10 g L^{-1} tryptone, 5 g L^{-1} yeast extract, and 10 g L^{-1} NaCl) medium containing 50 μg mL^{-1} kanamycin and grown overnight at 37 °C with shaking at 225 rpm. Next day, the overnight culture was inoculated 1:100 ml into fresh LB medium containing 50 μg mL^{-1} kanamycin and grown at 37 °C until the optical density at 600 nm (OD600) reached to 0.4. At this point, protein expression was induced by 100 μl of 1 M isopropyl-β-thiogalactopyranoside (IPTG) to give a final concentration of 1 mM. The induced culture was continued for 4 h and then processed for protein extraction.

2.4.2. Cell lysis and protein extraction

Bacterial cells were harvested by centrifugation at 4000 rpm, 4 °C for 10 min. Supernatant was aspirated off and cells were washed three times with cold binding-wash solution (20 mM Na_2HPO_4, pH = 7.0). The cells were then re-suspended in 2 ml cold lysis buffer (20 mM Na_2HPO_4, 10 mM imidazole, pH = 7.0). Cell lysis was further continued by sonication on ice (15 s at 70% power, four times, 1 min intervals with a M73 probe). The lysate was centrifuged at 12000 rpm, 4 °C for 10 min to remove the crude precipitates. Supernatant was then filtered through a 0.2 μm cellulose acetate filter (Millipore, USA) as soluble cell extract (SCE).

2.4.3. Protein purification by $MnFe_2O_4$@SiO_2@Ni-Salen complex MNPs

At first, 5 mg of $MnFe_2O_4$@SiO_2@Ni-Salen complex MNPs in stable powdery form were transferred into the eppendorf tubes, washed, and equilibrated three times with 500 μl cold lysis buffer. After each pipetting and mixing, tube was placed on a magnet until the beads migrated to the side of the tube and the clarified liquids were discarded. Meanwhile, 800 μl SCE were diluted with 200 μl cold lysis buffer before mixing with beads. The mixture mixed well by gentle pipetting and incubated for 30 min on a roller mixer for protein binding. After the binding process, the tubes were placed in the magnetic separator and except a small volume (30 μl) of the clarified supernatant which was collected and frozen for further analysis as flow through samples (FT); the rest was removed and discarded. The washing steps were performed four times by adding 500 μl wash buffer (50 mM NaH_2PO_4, 300 mMNaCl, 10 mM imidazole, pH = 8.0) to remove nonspecifically-adsorbed proteins. At each washing step, a small portion of supernatant was collected ($W_{1\text{-}4}$) and the rest was discarded. After four washing steps, the entrapped histidine-tagged proteins were eluted with 200 μl elution buffer (50 mM NaH_2PO_4, 300 mM NaCl containing 100 or 250 mM imidazole, pH 8.0). Supernatant from each elution step (E1-5) was then collected and stored at −20 °C. Thirty μl of all collected samples including SCE, FT, W1-4 and E1-5 were mixed with 7 μl of loading buffer (50 mM Tris-HCl pH 6.8, 10% glycerol, 2.5% SDS, 0.1% bromophenol blue, 25 mM Dithiothreitol), boiled for three minutes and subjected to sodium dodecyl sulfate–polyacrylamide gel electrophoresis (SDS-PAGE).

2.4.4. Western blotting

After separation on SDS-PAGE gel, proteins were transferred to nitrocellulose membranes (Hybond-ECL; Amersham, Sweden) in 100 mM Tris-HCl pH 7.5, containing 2.5 M NaCl, 0.5% Tween 20, 2% Triton X-100 and 20% (v/v) methanol, for 1 h at 1 mA/cm^2, using a Bio-Rad apparatus (Berkeley, California, USA). To detect proteins, membranes were blocked in bovine serum albumin (BSA) 5% for 3 h followed by incubation for 1 h at 4 °C with a horseradish peroxidase (HRP)-conjugated monoclonal anti-His antibody at a 1:100,000 dilution. Membranes were developed with ECL detection kit according to the manufacturer's instruction (Hybond-ECL; Amersham, Sweden).

2.4.5. Determination of physical parameters of $MnFe_2O_4$@SiO_2@Ni-Salen complex MNPs for protein purification

Physical parameters of the prepared MNPs including percent of specific binding capacity, yield and recovery were determined as we described elsewhere [48] by a densitometry method. The method of densitometry we employed was based on calculation of AUC (area under curve) which was based on both band density (height of the curve) and band area (width of the curve). In brief, specific binding capacity of the matrix was calculated as percent of desired band density in flow through fraction subtracted from 100%. Yield of the matrix was defined as the sum of the percents of the specific band densities at four elution steps (E1-4). Recovery was also calculated as the percent of purification yield divided by specific binding capacity. For determining MNPs binding capacity (mg/g MNPs), collective protein content in eluted fractions was measured photometrically having known the absorptivity of protein-A to be 1.65 according to the Beer-Lambert law. The results were obtained from four different individual tests and expressed as mean ± SD.

3. Results and discussion

In this research, we first synthesized 2-(((3-(trimethoxysilyl)-propyl)imino)methyl) phenol. The salen ligand was prepared from

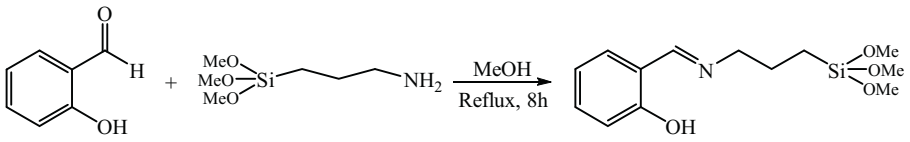

Fig. 1. Preparation of 2-(((3-(trimethoxysilyl)propyl)imino)-methyl)phenol from condensation reaction of salicylaldehyde and 3-aminopropyl (trimethoxy) silane.

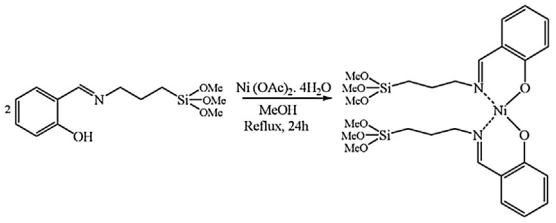

Fig. 2. Preparation of Ni-Salen complex via the reaction of Schiff base ligand with $Ni(OAc)_2{\cdot}4H_2O$ in 2:1 molar ratio.

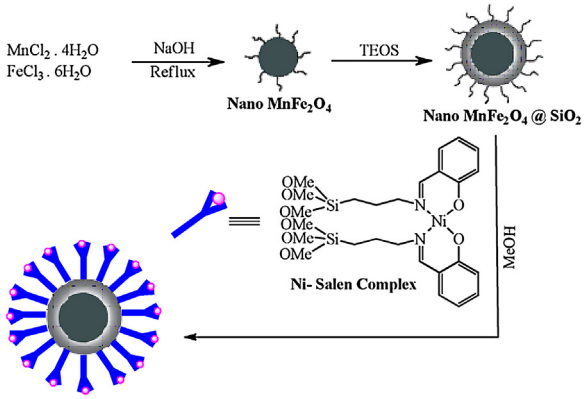

Fig. 3. Preparation of $MnFe_2O_4$@SiO_2@Ni-Salen complex as a result of reaction between prepared Ni-Salen complex with silica-supported $MnFe_2O_4$ nanoparticles.

the reaction of salicylaldehyde with APTMS in 1:1 molar ratio in methanol under reflux condition for 8 h. (Fig. 1).

At the next step, Schiff base complex was prepared by treating the above mentioned Schiff base ligand with $Ni(OAc)_2{\cdot}4H_2O$ in 2:1 molar ratio in methanol under reflux condition (Fig. 2).

The structure of products was characterized by physical and spectroscopic investigations. FT-IR spectrum of the Schiff base exhibited a band at 1634 cm^{-1} assignable to C=N of azomethine. This band shifted to lower region and appeared in 1620 cm^{-1} because of coordination of the nitrogen atom with Ni(II) indicating complexation of imine group. The OH stretching frequency was appeared at around 3331–3353 cm^{-1} with particular width and some bands at 1400–1500 cm^{-1} assigned to stretching vibrations of aromatic rings. In the ^1H NMR spectrum, the broad signal at 13.2 ppm was assigned to the proton of the hydroxyl group. The proton of HC=N has chemical shift in $\delta = 8.5$ ppm. The aromatic protons exhibited multiplet in the region $\delta = 7.33–7.80$ ppm with four integral values. The signals around $\delta = 0.83–1.80$ ppm with six integral values were assigned to the protons of CH_2 groups [41].

Finally, in order to prepare functionalized nanoparticles, salen complex of Ni(II) was supported on $MnFe_2O_4$@SiO_2 nanoparticles. This protocol has been illustrated in Fig. 3. Superparamagnetic manganese ferrite nanoparticles were synthesized by a co-precipitation method in basic aqueous medium [38]. The coating process was performed by suspending the MNPs in an ethanol–water solution and mixing with TEOS to form a silica shell [39]. Then, the prepared Ni-Salen complex was immobilized on the surface of $MnFe_2O_4$@SiO_2 in methanol solution under reflux condition. Characterization of the prepared MNPs was performed with different physicochemical methods such as; Fourier Transform Infrared (FT-IR) spectroscopy, X-ray diffraction (XRD), Scanning Electron Microscopy (SEM), Vibrating Sample Magnetometry (VSM), Thermo Gravimetric analysis (TGA), and Energy Dispersive X-rays (EDX) analysis.

3.1. Characterization of the catalyst

3.1.1. FT-IR spectra

S1 in supporting information shows the FT-IR spectra of the samples including $MnFe_2O_4$, $MnFe_2O_4$@SiO_2 and $MnFe_2O_4$@SiO_2@Ni-Salen complex. In S1 (a) (supporting information), the band at 584 cm^{-1} were assigned to the vibration of the Fe—O. In addition, there were obvious peaks at 3427 cm^{-1} and 1630 cm^{-1} that could be attributed to —OH groups [41]. In compared to the curve a, the curve b shows the Si—O—Si stretching of the silica layer appeared as a strong peak at 1100 cm^{-1} [42]. For $MnFe_2O_4$@SiO_2@Ni-Salen complex (S1 (c); supporting information), two obvious bands at 2925 cm^{-1} and 2860 cm^{-1} were observed which were assigned to C—H stretching. Some weak bands at 1400–1500 cm^{-1} assigned to stretching vibrations of C=C bands in aromatic ring. The C=N stretch of the imine was appeared at 1618 cm^{-1} due to the coordination of the nitrogen with Ni (II). FT-IR spectra confirmed the modification of $MnFe_2O_4$@SiO_2@Ni-Salen complex through the obvious peaks.

3.1.2. X-ray diffraction (XRD)

The crystalline structure of the synthesized $MnFe_2O_4$, $MnFe_2O_4$@SiO_2 and $MnFe_2O_4$@SiO_2@Ni-Salen complex was determined by X-ray diffraction (XRD) (S2; supporting information). In the 2Θ of 20–80°, six characteristic peaks for $MnFe_2O_4$ ($2\theta = 29.94°$, 35.24°, 42.75°, 52.94°, 56.42°, and 61.86°) were observed for three samples. The peak positions at the corresponding 2θ were indexed as (220), (311), (400), (331), (422), and (333) respectively, which matched well with the database for magnetite in the JCPDS-International center for diffraction data (JCPDS 1964-73) file.

3.1.3. Scanning electron microscopy (SEM)

S3 in supporting information depicts SEM images MNPs. $MnFe_2O_4$ particles were found to be spherical with particle size in a mean diameter of about 30–35 nm (a). $MnFe_2O_4$@SiO_2@Ni-Salen complex nanoparticles were nearly spherical with average size of 70–85 nm (b). Therefore, coating of MNPs with Schiff base complex did not seem to significantly affect morphology of MNPs.

3.1.4. Vibrating sample magnetometry (VSM)

Vibrating sample magnetometry (VSM) was employed to study the magnetic properties of the synthesized MNPs. The magnetic hysteresis loops of the samples at room temperature are illustrated in S4 (supporting information). The saturation magnetization value of pure $MnFe_2O_4$ at room temperature was 56 emu g^{-1} which was decreased to about 36 emu g^{-1} after coupling with Schiff base complex. Since no remanence remained when the external magnetic field was removed, it could be concluded that both $MnFe_2O_4$ and $MnFe_2O_4$@SiO_2@Ni-Salen complex had superparamagnetic nature at room temperature. Such characteristic is important because

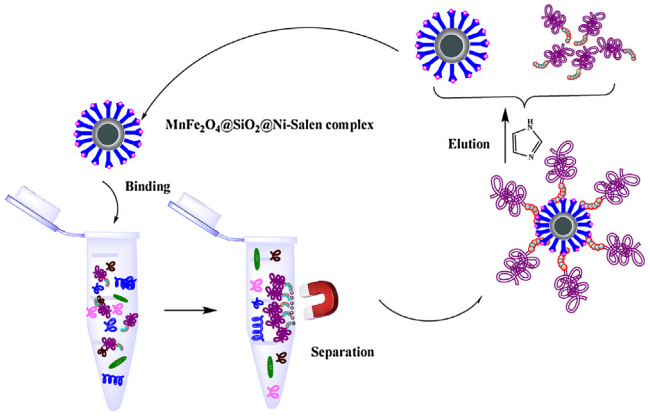

Fig. 4. Schematic representation of 6 × His-tagged protein-A separation from crude *E. Coli* lysate using $MnFe_2O_4$@SiO_2@ Ni-Salen complex MNPs in three steps: binding (1), separation (2) and elution (3).

it prevents aggregation of the particles and enables them to re-disperse rapidly in the solution. In the absence of an external magnetic field, the synthesized MNPs exhibited a stable dark homogeneous solution with excellent dispersity. However, when an external magnetic field was applied; nanoparticles were attracted to the wall of the vial and the solution became completely clear and transparent.

3.1.5. Thermo gravimetric analysis (TGA)

Differential thermal analysis (DTA) measurements of the complex showed an endothermic peak at low temperature (lower than 200 °C) and an exothermic peak between 200 and 600 °C (S5, supporting information). Thermogravimetric analysis (TGA) of the $MnFe_2O_4$@SiO_2@Ni-Salen MNPs supported above data on endothermic peak to be below 200 °C which is attributed to the weight loss of MNPs (7%) due to release of physisorbed water molecules on the surface of the complex. The exothermic peak accompanied with a 5% mass loss in the temperature range of 200–600 °C. Through the TGA analysis, the content of ligand in $MnFe_2O_4$@SiO_2@Ni-Salen complex was estimated to be 0.15 mmol g^{-1}.

3.1.6. Energy dispersive X-rays (EDX) analysis

By ICP analysis, Ni content in the $MnFe_2O_4$@SiO_2@Ni-Salen complex was determined to be 0.38 mmol g^{-1}. Elemental composition of prepared MNPs was further analyzed by energy dispersive X-rays (EDX) analysis showing the presence of C, N, Mn, Si, O, Fe and Ni (S6, supporting information).

3.2. Purification of 6 × His-tagged proteins

The separation process of 6 × histidine-tagged recombinant protein-A from crude *E. coli* lysate is illustrated in Fig. 4. In a typical experiment, $MnFe_2O_4$@SiO_2@Ni-Salen complex MNPs were added to the SCE at room temperature for 30 min and then separated from the solution by applying an external magnet. The physically adsorbed proteins or residual protein solution were removed by washing processes. Then, attached 6 × histidine-tagged recombinant protein-A was released from MNPs by imidazole. The prepared nanoparticles showed excellent binding selectivity (Fig. 5) and capacity (Fig. 6) for 6 × histidine-tagged recombinant protein-A.

Fig. 5(A) illustrates representative result of SDS-PAGE analysis of purified 6 × histidine-tagged recombinant protein-A from *E.coli*cell lysate by $MnFe_2O_4$@SiO_2@Ni-Salen complex MNPs. Analysis of SCE revealed over expression of recombinant protein-A (42 kD). Binding efficacy of the recombinant protein on prepared

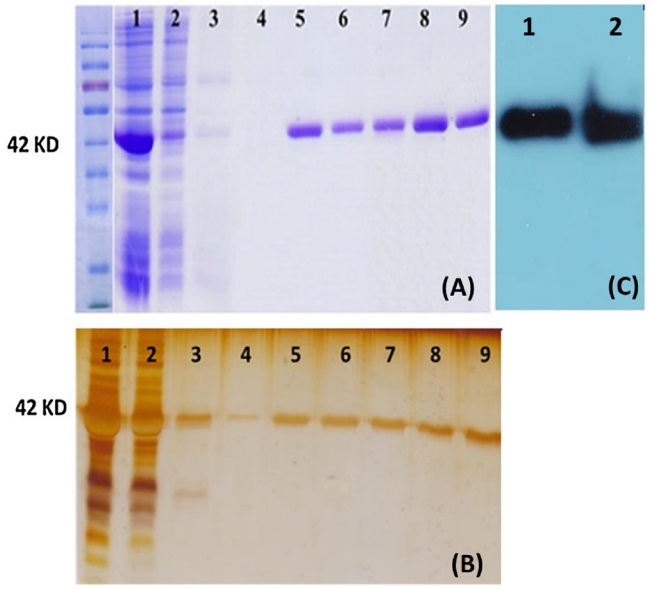

Fig. 5. Characterization of 6 × histidine-tagged protein-A purified by $MnFe_2O_4$@SiO_2@Ni-Salen complex. A and B: SDS-PAGE and Silver staining, respectively. Lane 1: SCE, Lane 2: Flow through, Lane 3: Wash 1, Lane 4: Wash 4, Lane 5–9: Eluates at imidazole concentrations of 100 (three elution steps) and 250 (two elution steps), respectively. (C) Lanes 1 and 2: Western blotting of purified protein-A using anti-his-tag antibody.

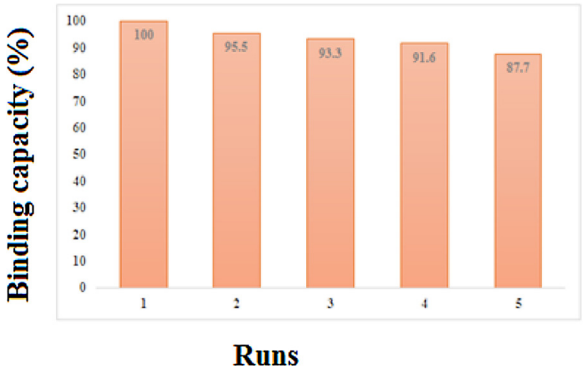

Fig. 6. Recycling capacity of the $MnFe_2O_4$@SiO_2@Ni-Salen complex MNPs for separation of 6 × histidine-tagged recombinant protein-A. The recyclability of $MnFe_2O_4$@SiO_2@Ni-Salen complex MNPs was evaluated by normalizing the binding capacity at each separation run in ratio to the first cycle.

MNPs was high as only tiny amount of target protein was lost in flow through and washing steps, while almost all non-specific proteins were removed after separation step (lane 2). The bound protein-A anchored to $MnFe_2O_4$@SiO_2@Ni-Salen complex MNPs through histidine tagged were eluted at the next step with increasing concentrations of imidazole. A single band of target protein was achieved at all elution steps denoting excellent selectivity of prepared MNPs (lanes 5–9). In order to confirm binding selectivity of $MnFe_2O_4$@SiO_2@Ni-Salen complex, the purity of the purified recombinant protein was tested with silver staining which has sensitivity in nanogram scale. As depicted in Fig. 5(B), silver staining of purified protein revealed a single band of target protein confirming the selectivity of the prepared MNPs. Western blot analysis with anti-histidine-tagged antibody also confirmed the identity of purified recombinant protein A. (Fig. 5(C)). The reactivity of purified protein A was also checked using indirect ELISA. Purified protein-A exhibited excellent reactivity with sheep immunoglobulin indicating functionality of the purified recombinant protein (data not shown).

Table 1
Physical parameters of the $MnFe_2O_4$@SiO_2@Ni-Salen complex MNPs.

Specific binding capacity (%)	Relative band density (%)					Yield (%)	Recovery (%)	Binding capacity (mg g^{-1})
	$E100_1$	$E100_2$	$E100_3$	$E250_1$	$E250_2$			
82.2	4	8.2	15.2	16.8	18.8	63	76	180 ± 15

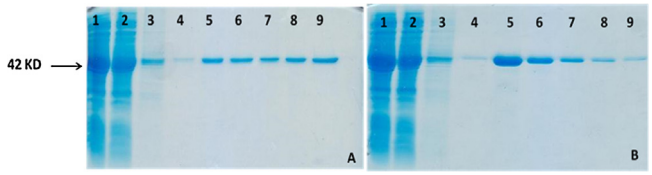

Fig. 7. SDS-PAGE analysis of 6 × histidine-tagged protein-A purified by $MnFe_2O_4$@SiO_2@Ni-Salen complex (A) and SiMAG/N-NTA/Nickel (B). Lane 1: SCE, Lane 2: Flow through, Lane 3: Wash 1, Lane 4: Wash 4, Lane 5–9: Elutes at imidazole concentrations of 100 (three elution steps) and 250 (two elution steps), respectively.

3.3. Reusability of the $MnFe_2O_4$@SiO_2@Ni-Salen complex MNPs

The recyclability of the $MnFe_2O_4$@SiO_2@Ni-Salen complex MNPs for separation of 6 × histidine-tagged recombinant protein was tested in five successive runs of protein-A separation (Fig. 6). After each separation, the MNPs were rinsed with strip buffer (100 mM EDTA, 500 mM NaCl, 20 mM Tris–HCl, pH 7.9) for three times to wash out the excess imidazole and to clean the surface of the particles. The recyclability of $MnFe_2O_4$@SiO_2@Ni-Salen complex MNPs was evaluated by normalizing the binding capacity of the matrix at each separation run in ratio to the binding capacity in the first cycle. We observed that the binding capacity of the synthesized $MnFe_2O_4$@SiO_2@Ni-Salen complex MNPs was decreased by about 13% after 5 runs of protein separation (Fig. 6), which could be attributed to the loss of a small fraction of matrix in each run of separation and also to residual protein fraction which remain in the matrix in spite of using high concentrations of imidazole. The latter could result in deactivation of a part of matrix active sites.

The purification selectivity of prepared MNPs was compared with commercially-available MNPs, SiMAG/N-NTA/Nickel (Chemicell, Berlin, Germany). As shown in Fig. 7, comparable selectivity was observed. However, target protein was released from our matrix in a stepwise manner by increasing imidazole concentration, while most of the attached protein to commercial matrix was eluted by stating concentration of imidazole. This result indicates higher affinity of recombinant protein to the matrix synthesized in this study.

3.4. Physical parameters of the $MnFe_2O_4$@SiO_2@Ni-Salen complex MNPs for protein purification

Physical parameters of the prepared MNPs including percent of specific binding capacity, Yield and recovery and also binding capacity (mg/g) were calculated by a densitometric method and corresponding results were expressed in Table 1.

Table 2 summarizes the binding capacity of other synthetic schemes for metal-chelating MNPs reported by other investigators for purification of different histidine-tagged proteins [43–47]. However, it should be noted that a frank judgment on comparative binding capacity of the MNPs presented here relative to those reported by others could not be merely made based on the results presented in Table 2; instead the nature of the recombinant protein may also be regarded as one important factor that influences this parameter.

Table 2
Comparison of binding capacity of some MNPs for purification of histidine-tagged recombinant proteins reported in the literature.

	Structure of beads	Binding Capacity (mg g^{-1})	Refs.
1	Fe_3O_4/Cys–Ni^{+2}	48.2	[43]
2	Ni-NTA-MNPs	146	[44]
3	Fe_3O_4/PMG/IDA–Ni^{2+}	103	[45]
4	Fe_3O_4/SiO_2-GPTMS-Asp-Co	9.45	[46]
5	Fe_3O_4/Au–ANTA–Co^{2+}	74	[47]
6	$MnFe_2O_4$@SiO_2@Ni-Salen complex	180	This work

4. Conclusion

In the present study, we developed a simple and inexpensive method for the preparation of a novel and efficient magnetic nanoparticle for purification of His-tag recombinant proteins. Our results clearly showed that these MNPs had excellent physical capabilities for protein purification including high efficiency, selectivity and capacity for the rapid purification of recombinant proteins. Indeed, prepared MNPs exhibited high recyclability and stability for purification of His-tagged proteins over several separation cycles which would facilitate their biomedical applications.

Acknowledgements

We are thankful to University of Kashan for supporting this work under grant number 159148/54, and to Avicenna Research Institute for providing equipment and laboratories for this research to be completed.

Appendix A. Supplementary data

Supplementary data associated with this article can be found, in the online version, at http://dx.doi.org/10.1016/j.chroma.2017.02.014.

References

[1] J. Porath, J. Carlson, I. Olsson, G. Belfrage, Metal chelate affinity chromatography, a new approach to protein fractionation, Nature 258 (1975) 598599.
[2] Current Protocols in Molecular Biology, in: R. Ausubel, R.E. Kingston, D.D. Moore, J.G. Seidman, K. Smith, L.M. Albright, D.M. Coen, A. Varki (Eds.), John Wiley & Sons, New York, 2003.
[3] R.G. Pearson, Hard and soft acids and bases, J. Am. Chem. Soc. 85 (1963) 3533–3539.
[4] S. Gibert, N. Bakalara, X. Santarelli, Three-step chromatographic purification procedure for the production of a His-tag recombinant kinesin over expressed in E. coli, J. Chromatogr. B 737 (2000) 143–150.
[5] R.J. Everson, H.E. Parker, Zinc binding and synthesis eight-hydroxy-quinoline-agarose, Bioinorg. Chem. 4 (1974) 15–20.
[6] J. Porath, B. Olin, Immobilized metal affinity adsorption and immobilized metal affinity chromatography of biomaterials. Serum protein affinities for gel-immobilized iron and nickel ions, Biochemistry 22 (1983) 1621–1630.
[7] N. Ramadan, J. Porath, Fe^{3+}-hydroxamate as immobilized metal affinity-adsorbent for protein chromatograph, J. Chromatogr. 321 (1985) 93–104.
[8] E. Sulkowski, Trends. Biotechnol. 3 (1985) 1–7.
[9] E. Sulkowski, Immobilized metal-ion affinity chromatography: Imidazole proton pump and chromatographic sequelae. I. Proton pump, J. Mol. Recognit. 9 (1996) 389–393.
[10] E. Hochuli, H. Doebeli, A. Schacher, New metal chelate adsorbent selective for proteins and peptides containing neighbouring histidine residues, J. Chromatogr. 411 (1987) 177–184.

[11] E. Hochuli, H. Dobeli, A. Schacher, New metal chelate adsorbent selective for proteins and peptides containing neighbouring histidine residues, J. Chromatogr. 411 (1987) 177–184.
[12] J. Kim, H.Y. Park, J. Kim, J. Ryu, D.Y. Kwon, R. Grailhe, R. Song, Ni–nitrilotriacetic acid-modified quantum dots as a site-specific labeling agent of histidine-tagged proteins in live cells, Chem. Commun. (2008) 1910–1912.
[13] R. Ahrends, S. Pieper, A. Kuhn, H. Weisshoff, M. Hamester, T. Lindemann, C. Scheler, K. Lehmann, K. Taubner, M.W. Linscheid, A metal-coded affinity tag approach to quantitative proteomics, Mol. Cell. Proteomics 6 (2007) 1907–1916.
[14] R. Ahrends, S. Pieper, B. Neumann, C. Scheler, M.W. Linscheid, Metal-coded affinity tag labeling: a demonstration of analytical robustness and suitability for biological applications, Anal. Chem. 81 (2009) 2176–2184.
[15] H. Block, B. Maertens, A. Spriestersbach, N. Brinker, J. Kubicek, R. Fabis, J. Labahn, F. Schafer, Immobilized-metal affinity chromatography (IMAC): a review, Methods Enzymol. 463 (2009) 439–473.
[16] K. Kracalıkova, G. Tishchenko, M. Bleha, Effect of the matrix structure and concentration of polymer-immobilized Ni^{2+}–iminodiacetic acid complexes on retention of IgG_1, J. Biochem. Biophys. Methods 67 (2006) 7–25.
[17] Y. Liao, Y. Cheng, Q. Li, Preparation of nitrilotriacetic acid/Co^{2+}-linked, silica/boron-coated magnetite nanoparticles for purification of 6 × histidine-tagged proteins, J. Chromatogr. A 1143 (2007) 65–71.
[18] R.J. Ghosh, Protein separation using membrane chromatography: opportunities and challenges, J. Chromatogr. A 952 (2002) 13–27.
[19] Z. Rashid, H. Naeimi, A.-H. Zarnani, M. Nazari, M.-R. Nejadmoghaddam, R. Ghahremanzadeh, Fast and highly efficient purification of 6 × histidine-tagged recombinant proteins by Ni-decorated $MnFe_2O_4$@SiO_2@NH_2@2AB as novel and efficient affinity adsorbent magnetic nanoparticles, RSC Adv. 6 (2016) 36840–36848.
[20] J. Meng, J.G. Walter, O. Kokpinar, F. Stahl, T. Scheper, Automated microscale his-tagged protein purification using Ni-NTA magnetic agarose beads, Chem. Eng. Technol. 31 (2008) 463–468.
[21] W.F. Ma, Y. Zhang, L.L. Li, L.J. You, P. Zhang, Y.T. Zhang, J.M. Li, M. Yu, J. Guo, H.J. Lu, C.C. Wang, Tailor-made magnetic Fe_3O_4@$mTiO_2$ microspheres with a tunable mesoporous anatase shell for highly selective and effective enrichment of phosphopeptides, ACS Nano 6 (2012) 3179–3188.
[22] J. Yang, C.H. Lee, J. Park, S. Seo, E.K. Lim, Y.J. Song, J.S. Suh, H.G. Yoon, Y.M. Huh, S.J. Haam, Superparamagnetic core-shell polymer particles for efficient purification of his-tagged proteins, Mater. Chem. 20 (2010) 8624–8630.
[23] B. Luo, S. Xu, A. Luo, W.R. Wang, S.L. Wang, J. Guo, Y. Lin, D.Y. Zhao, C.C. Wang, Mesoporous biocompatible and acid-degradable magnetic colloidal nanocrystal clusters with sustainable stability and high hydrophobic drug loading capacity, ACS Nano 5 (2011) 1428–1435.
[24] D. Li, J. Tang, C. Wei, J. Guo, S.L. Wang, D. Chaudhary, C.C. Wang, Doxorubicin-Conjugated mesoporous magnetic colloidal nanocrystal clusters stabilized by polysaccharide as a smart anticancer drug vehicle, Small 8 (2012) 2690–2697.
[25] H.S. Cho, Z.Y. Dong, G.M. Pauletti, J.M. Zhang, H. Xu, H.C. Gu, L.M. Wang, R.C. Ewing, C. Huth, F. Wang, D.L. Shi, Fluorescent, superparamagnetic nanospheres for drug storage, targeting, and imaging: a multifunctional nanocarrier system for cancer diagnosis and treatment, ACS Nano 4 (2010) 5398–5404.
[26] S. Nikoo, M. Ebtekar, M. Jeddi-Tehrani, A. Shervin, M. Bozorgmehr, S. Kazemnejad, A.H. Zarnani, Effect of menstrual blood-derived stromal stem cells on proliferative capacity of peripheral blood mononuclear cells in allogeneic mixed lymphocyte reaction, J. Obstet. Gynaecol. Res. 38 (2012) 804–809.
[27] S. Kazemnejad, M.M. Akhondi, M. Soleimani, A.H. Zarnani, M. Khanmohammadi, S. Darzi, K. Alimoghadam, Characterization and chondrogenic differentiation of menstrual blood-derived stem cells on a nanofibrous scaffold, Int. J. Artif. Organs 35 (2012) 55–66.
[28] M. Zhang, X.W. He, L.X. Chen, Y.K. Zhang, Preparation of IDA-cufunctionalized core–satellite Fe_3O_4/polydopamine/aumagnetic nanocomposites and their application for depletion of abundant protein in bovine blood, J. Mater. Chem. 20 (2010) 10696–10704.
[29] Q. Jian, Y.X. Liu, X.W. He, L.X. Chen, Y.K. Zhang, Click chemistry: a new facile and efficient strategy for the preparation of Fe_3O_4nanoparticles covalently functionalized with IDA-Cu and their application in the depletion of abundant protein in blood samples, Nanoscale 4 (2012) 6336–6342.
[30] R. Di Corato, P. Piacenza, M. Musaro, R. Buonsanti, P.D. Cozzoli, M. Zambianchi, G. Barbarella, R. Cingolani, L. Manna, T. Pellegrino, Magnetic–fluorescent colloidal nanobeads: preparation and exploitation in cell separation experiments, Macromol. Biosci. 9 (2009) 952–958.
[31] M.I. Shukoor, F. Natalio, H.A. Therese, M.N. Tahir, V. Ksenofontov, M. Panthofer, M. Eberhardt, P. Theato, H.C. Schroder, W.E.G. Muller, W. Tremel, Fabrication of a silica coating on magnetic γ-Fe_2O_3 nanoparticles by an immobilized enzyme, Chem. Mater. 20 (2008) 3567–3573.
[32] F. Xu, J.H. Geiger, G.L. Baker, M.L. Bruening, Polymer brush-modified magnetic nanoparticles for His-tagged protein purification, Langmuir 27 (2011) 3106–3112.
[33] X. Zou, K. Li, Y. Zhao, Y. Zhang, B. Li, C. Song, Ferroferric oxide/L-cysteinemagneticnanospheres for capturing histidine-tagged proteins, J. Mater. Chem. B 1 (2013) 5108–5113.
[34] Y. Wang, G. Wang, Y. Xiao, Y. Yang, R. Tang, Yolk–shell nanostructured Fe_3O_4@$NiSiO_3$ for selective affinity and magnetic separation of His-tagged proteins, ACS Appl. Mater. Interfaces 6 (2014) 19092–19099.
[35] F. Xu, J.H. Geiger, G.L. Baker, M.L. Bruening, Polymer brush-modified magnetic nanoparticles for His-tagged protein purification, Langmuir 27 (2011) 3106–3112.
[36] H.Y. Xie, R. Zhen, B. Wang, Y.J. Feng, P. Chen, J. Hao, Fe_3O_4/Au core/shell nanoparticles modified with $Ni2^+$-nitrilotriacetic acid specific to Histidine-tagged proteins, J. Phys. Chem. C 114 (2010) 4825–4830.
[37] B. Weber, E.-G. Jäger, Structure and magnetic properties of iron (II/III) complexes with $N_2O_2^2$–coordinating schiff base like ligands, Eur. J. Inorg. Chem. (2009) 465–477.
[38] H. Aijun, L. Juanjuan, Y. Mingquan, L. Yan, P. Xinhua, Preparation of Nano-$MnFe_2O_4$ and its catalytic performance of thermal decomposition of ammonium perchlorate, Chin. J. Chem. Eng. 19 (2011) 1047–1051.
[39] B. Sahoo, S.K. Sahu, S. Nayak, D. Dhara, P. Pramanik, Catal. Sci. Technol. 2 (2012) 1367.
[40] J. Butler, Y. Zhao, M. Sinkora, N. Wertz, I. Kacskovics, Immunoglobulins, antibody repertoire and B cell development, Dev. Comp. Immunol. 33 (2009) 321–333.
[41] F. Dehghani, A.R. Sardarian, M. Esmaeilpour, Salen complex of Cu(II) supported on superparamagnetic Fe_3O_4@SiO_2 nanoparticles: an efficient and recyclable catalyst for synthesis of 1- and 5-substituted 1H-tetrazoles, J. Organomet. Chem. 743 (2013) 87–96.
[42] P. Rattanaburi, B. Khumraksa, M. Pattarawarapan, Synthesis and applications of Fe_3O_4-diisopropylaminoacetamide as a versatile and reusable magnetic nanoparticle supported *NN*-diisopropylethylamine equivalent, Tetrahedron Lett. 53 (2012) 2689–2693.
[43] X. Zou, K. Li, Y. Zhao, Y. Zhang, B. Li, C. Song, Ferroferric oxide/L-cysteinemagnetic nanospheres for capturing histidine-tagged proteins, J. Mater. Chem. B 1 (2013) 5108–5113.
[44] W. Wang, D.I.C. Wang, Z. Li, Facile fabrication of recyclable and active nanobiocatalyst: purification and immobilization of enzyme in one pot with Ni-NTA functionalized magnetic nanoparticle, Chem. Commun. 47 (2011) 8115–8117.
[45] Y. Zhang, Y. Yang, W. Ma, J. Guo, Y. Lin, C. Wang, Uniform magnetic core/shell microspheres functionalized with Ni^{2+}–Iminodiacetic acid for one step purification and immobilization of His-tagged enzymes, ACS Appl. Mater. Interfaces 5 (2013) 2626–2633.
[46] G. Fenga, D. Hu, L. Yang, Y. Cui, X. Cui, H. Li, Immobilized-metal affinity chromatography adsorbent with paramagnetism and its application in purification of histidine-tagged proteins, Sep. Purif. Technol. 74 (2010) 253–260.
[47] L. Zhang, X. Zhu, D. Jiao, Y. Sun, H. Sun, Efficient purification of His-tagged protein by superparamagnetic Fe_3O_4/Au–ANTA–Co^{2+} nanoparticles, Mater. Sci. Eng. C 33 (2013) 1989–1992.
[48] M.R. Nejadmoghaddam, M. Chamankhah, S. Zarei, A.H. Zarnani, Profiling and quantitative evaluation of three nickel-coated magnetic matrices for purification of recombinant proteins: helpful hints for theoptimized nanomagnetic sable matrix preparation, J. Nanobiotechnol. 9 (2011) 31–42.